

## Synthesis and Characterization of a Bisadduct of La@C<sub>82</sub>

Lai Feng,<sup>†</sup> Takahiro Tsuchiya,<sup>†</sup> Takatsugu Wakahara,<sup>†</sup> Tsukasa Nakahodo,<sup>†</sup> Qiuyue Piao,<sup>†</sup> Yutaka Maeda,<sup>‡</sup> Takeshi Akasaka,<sup>\*,†</sup> Tatsuhisa Kato,<sup>¶</sup> Kenji Yoza,<sup>\*,#</sup> Ernst Horn,<sup>⊥</sup> Naomi Mizorogi,<sup>§</sup> and Shigeru Nagase<sup>\*,§</sup>

Center for Tsukuba Advanced Research Alliance, University of Tsukuba, Tsukuba 305-8577, Japan, Department of Chemistry, Tokyo Gakugei University, Koganei 184-5801, Japan, Department of Chemistry, Josai University, Sakado 350-0295, Japan, Bruker AXS K. K., Yokohama 221-0022, Japan, Department of Chemistry, Rikkyo University, Tokyo 171-8501, Japan, and Department of Theoretical Molecular Science, Institute for Molecular Science, Okazaki 444-8585, Japan

Received December 11, 2005; E-mail: akasaka@tara.tsukuba.ac.jp; nagase@ims.ac.jp

Endohedral metallofullerenes (EMFs) encapsulate one or more metal atoms inside a hollow fullerene cage.<sup>1</sup> Since the paramagnetic Y@C<sub>82</sub> was observed to form a dimer on the Cu(111) surface in the STM image, the dimerization of paramagnetic EMFs has attracted considerable interest.<sup>1,2</sup> The unpaired electron of Y@C<sub>82</sub> was considered as a driving force for the dimerization. However, no direct evidence has been reported for the dimer formation of EMFs so far. Meanwhile, diverse monoadducts of EMFs have been synthesized and structurally characterized.<sup>3</sup> In contrast, only very limited studies have been carried out for the multiaddition of EMFs,<sup>4</sup> though more widely potential applications in biomedical and material science can be expected for the multiadducts.<sup>5</sup> Herein, we report a well-defined bisadduct of La@C<sub>82</sub> (C<sub>2v</sub>), which was prepared by a Bingel–Hirsch reaction.<sup>6</sup> This bisaddition proceeded in a highly regioselective way and led to the dominant formation of one bisadduct isomer (**A**) in a good yield. As the first unambiguous example of the dimer formation of EMFs, it is verified by X-ray crystallographic analysis that **A** forms a dimer in the single crystal.

Very recently, we have reported the reaction of La@C<sub>82</sub> with bromomalonate in the presence of 1,8-diazabicyclo[5.4.0]undec-7-ene (DBU) (Bingel–Hirsch reaction), which yields a singly bonded monoadduct as the major product.<sup>7</sup> However, the reaction of La@C<sub>82</sub> with malonate in the presence of DBU proceeded very slowly at room temperature. This may be ascribed to the lower acidity of the methylene protons of malonate. When the temperature was increased up to 60 °C, the reaction proceeded much faster and finished in a few hours.

As Figure 1 shows, the major product of the reaction of La@C<sub>82</sub> with malonate was eluted with the retention time of 7.6–8.0 min and was separated readily from other adducts and unreacted starting materials by one-step HPLC separation. The isolated fraction showed only one peak on all available columns, indicating that only one isomer exists in the fraction. Further analysis by MALDI-TOF mass spectroscopy on the fraction exhibits a molecular ion peak at *m/z* 1441, suggesting that a bisadduct is formed, which is described as La@C<sub>82</sub>[CH(COOC<sub>2</sub>H<sub>5</sub>)<sub>2</sub>]<sub>2</sub> (**A**). Another weak peak is observed at *m/z* 1281, which is assignable to the fragment due to the loss of one malonate group.

The ESR and UV–visible–NIR spectra of the isolated **A** are shown in Figure 2. The *g* value (*g* = 2.0011), hyperfine coupling constant (*hfc* = 1.195 G), and peak-to-peak line widths ( $\Delta H_{pp}$  =

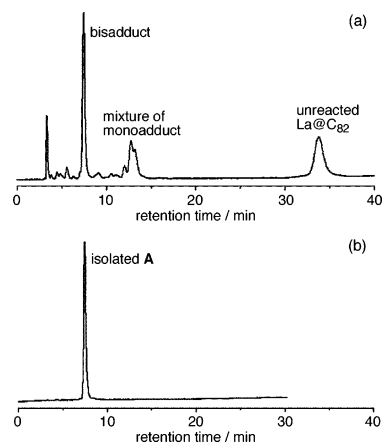


**Figure 1.** HPLC profiles for (a) reaction mixture and (b) isolated bisadduct **A** on Buckyprep column.

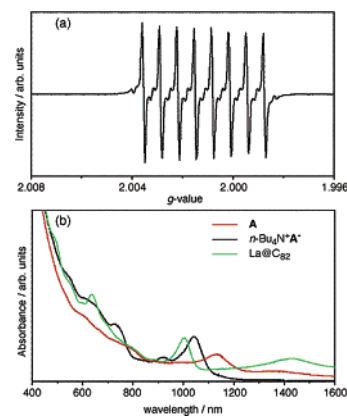


**Figure 2.** (a) ESR spectrum of bisadduct **A**; (b) UV–visible–NIR spectra of **A**, and *n*-Bu<sub>4</sub>N<sup>+</sup>A<sup>-</sup> and La@C<sub>82</sub>.

0.571 G) are close to those of the parent La@C<sub>82</sub> (*g* = 2.0011, *hfc* = 1.152 G, and  $\Delta H_{pp}$  = 0.360 G). However, the absorption spectrum of **A** is very different from that of La@C<sub>82</sub>. Bisadduct **A** shows a characteristic near-IR band at 1135 nm and an absorption onset around 1600 nm. These results suggest that **A** has a larger HOMO–LUMO gap than the pristine La@C<sub>82</sub>, even though it still retains an open-shell structural feature.

As Figure 3 shows, **A** crystallizes to form a dimer at 90 K.<sup>8</sup> As is obvious from the single-crystal structure, the addition of bromomalonate takes place at the C7 and C13 atoms of La@C<sub>82</sub> (C<sub>2v</sub>), providing bisadduct **A**. The C7 and C13 atoms are located at the apex of two hexagons and one pentagon. Notably, C7 is also

<sup>†</sup> University of Tsukuba.

<sup>‡</sup> Tokyo Gakugei University.

<sup>¶</sup> Josai University.

<sup>#</sup> Bruker AXS K. K.

<sup>⊥</sup> Rikkyo University.

<sup>§</sup> Institute for Molecular Science.

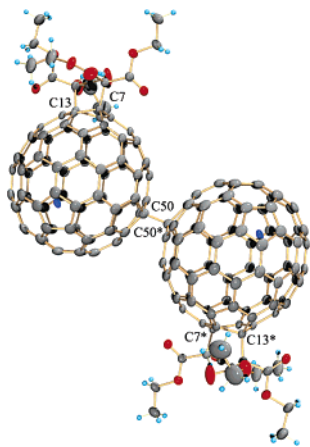


**Figure 3.** ORTEP drawing of the dimer of bisadduct **A**. Only one La site with the highest occupancy is shown. The hexane molecules are omitted for clarity.

**Table 1.** Redox Potentials (V)<sup>a</sup> of La@C<sub>82</sub> and Bisadduct **A**

compound	<sup>ox</sup> E <sub>1</sub>	<sup>red</sup> E <sub>1</sub>	<sup>red</sup> E <sub>2</sub>	<sup>red</sup> E <sub>3</sub>
La@C <sub>82</sub>	0.07	-0.42	-1.37	-1.53
<b>A</b>	0.08	-0.32	-1.57	

<sup>a</sup> Versus Fc/Fc<sup>+</sup>. In *o*-dichlorobenzene with 0.1 M (*n*-Bu)<sub>4</sub>NPF<sub>6</sub> at a Pt working electrode. Values are obtained by DPV: pulse amplitude, 50 mV; scan rate, 20 mV s<sup>-1</sup>.

the addition site for the previously reported Bingel monoadduct of La@C<sub>82</sub> (C<sub>2v</sub>),<sup>7</sup> which strongly suggests that these Bingel bisadducts and monoadducts are formed via a similar formation mechanism. Interestingly, unlike other monoadducts of La@C<sub>82</sub>,<sup>3b,7</sup> several sites for the La atom have been identified on the C<sub>82</sub> cage of **A**. These sites are all in the neighborhood of the six-membered ring that is far from malonate. In La@C<sub>82</sub> (C<sub>2v</sub>), the La atom is situated on the C<sub>2</sub> axis. The La position in **A**, which has the most abundant occupancy (0.75), is off the C<sub>2</sub> axis and moves toward the hemisphere that undergoes bisaddition. Moreover, there exists a pair of enantiomers for **A**, which couple with each other at C50 and C50\* to form a dimer in the single crystal. The C50–C50\* bond (1.638(9) Å) is considerably longer than the typical C<sub>sp3</sub>–C<sub>sp3</sub> bond (1.54 Å) as well as the intercage C–C bond in other singly bonded fullerene dimers, such as (C<sub>60</sub>–C<sub>60</sub>)<sup>2-</sup> (1.597(7) Å),<sup>9a,b</sup> (C<sub>70</sub>–C<sub>70</sub>)<sup>2-</sup> (1.584(9) Å),<sup>9c</sup> RC<sub>60</sub>–C<sub>60</sub>R (1.576(6) Å),<sup>10</sup> and (Ar<sub>5</sub>C<sub>60</sub>–C<sub>60</sub>Ar<sub>5</sub>)<sup>4-</sup> (1.577(11) Å).<sup>11</sup> This may suggest that the intercage C–C bond in the dimer of **A** is considerably weaker.

Spin densities and POAV values<sup>12</sup> of **A** were calculated with hybrid density functional theory at the B3LYP level (LANL2DZ for La and 6-31G(d) for other atoms).<sup>13</sup> The C50 atom of **A** has a relatively high spin density and POAV value. In addition, the attaching malonate is not a steric hindrance for the dimerization at C50, though it is the large hindrance for other carbon atoms nearer the attachment, which possess somewhat higher spin densities and POAV values. Therefore, it may not be surprising that C50 is the most favored position for dimerization. It is interesting that the intercage C50–C50\* distance of 1.635 Å calculated for the dimer of **A** agrees very well with the experimental value of 1.638(9) Å.

Table 1 shows the redox potentials of **A** obtained from differential pulse voltammetry (DPV). Its first oxidation potential (<sup>ox</sup>E<sub>1</sub>) of 0.08 V is very close to the value of 0.07 V for La@C<sub>82</sub>, while its first reduction potential (<sup>red</sup>E<sub>1</sub>) shifted positively by 100 mV relative to the value for La@C<sub>82</sub>. Furthermore, **A** exhibits perfectly reversible behaviors for its first redox processes, as revealed by

further studies on cyclic voltammetry (CV). These suggest that **A** is stable toward oxidation and reduction under argon atmosphere on the CV time scale. The anion of **A** has been prepared by controlled potential electrolysis under argon. Its absorption profile is shown in Figure 2b. However, the anion is very sensitive to air and oxidized quickly. Its NMR measurement was unsuccessful due to its poor stability in air atmosphere.

In conclusion, the 7,13-bisadduct (**A**) of La@C<sub>82</sub> (C<sub>2v</sub>) has been synthesized in a good yield by a Bingel–Hirsch reaction. Its structure has been well-defined by X-ray crystallographic analysis. A pair of enantiomers of this bisadduct form a dimer in the single crystal. This is noticeable as the first direct observation of the dimer of EMF derivatives, which provides basic information for further studies on the dimerization of EMFs.<sup>14</sup>

**Acknowledgment.** F.L. thanks the Japan Society for the Promotion of Science (JSPS) for the postdoctoral fellowship for foreign researchers. This work is supported in part by a Grant-in-Aid for Nanotechnology Supporting Program from the Ministry of Education, Culture, Sports, Science and Technology of Japan.

**Supporting Information Available:** Complete refs 3b–e and 7, experimental section, HPLC profile, CV and DPV spectrum of **A**. X-ray crystallographic data of **A** in CIF format at 90 K. This material is available free of charge via the Internet at <http://pubs.acs.org>.

## References

- (1) *Endofullerenes: A New Family of Carbon Cluster*; Akasaka, T., Nagase, S., Eds.; Kluwer Academic Publisher: Dordrecht, The Netherlands, 2002.
- (2) Sakurai, T.; Wang, X.; Xue, Q.; Hasegawa, Y.; Hashizume, T.; Shinohara, H. *Prog. Surf. Sci.* **1996**, *51*, 263–408.
- (3) (a) Iezzi, E. B.; Duchamp, J. C.; Harish, K.; Glass, T. E.; Lee, H. M.; Olmstead, M. M.; Balch, A. L.; Dorn, H. C. *J. Am. Chem. Soc.* **2002**, *124*, 524–525. (b) Maeda, Y.; et al. *J. Am. Chem. Soc.* **2004**, *126*, 6858–6859. (c) Nikawa, H.; et al. *J. Am. Chem. Soc.* **2005**, *127*, 9684–9685. (d) Iiduka, Y.; et al. *J. Am. Chem. Soc.* **2005**, *127*, 9956–9957. (e) Yamada, M.I. et al. *J. Am. Chem. Soc.* **2005**, *127*, 14570–14571. (f) Cardona, C. M.; Kitaygorodskiy, A.; Ortiz, A.; Herranz, M. A.; Echegoyen, L. *J. Org. Chem.* **2005**, *70*, 5092–5097. (g) Cardona, C. M.; Kitaygorodskiy, A.; Echegoyen, L. *J. Am. Chem. Soc.* **2005**, *127*, 10448–10453.
- (4) (a) Stevenson, S.; Stephen, R. R.; Amos, T. M.; Cadorette, V. R.; Reid, J. E.; Phillips, J. P. *J. Am. Chem. Soc.* **2005**, *127*, 12776–12777. (b) Kareev, I. E.; Lebedkin, S. F.; Bubnov, V. P.; Yagubskii, E. B.; Ioffe, I. N.; Khavrel, P. A.; Kuvychko, I. V.; Strauss, S. H.; Boltalina, O. V. *Angew. Chem., Int. Ed.* **2005**, *44*, 1846–1849. (c) Tagmatarchis, N.; Taninaka, A.; Shinohara, H. *Chem. Phys. Lett.* **2002**, *355*, 226–232.
- (5) (a) Tóth, E.; Bolskar, R. D.; Borel, A.; González, G.; Helm, L.; Merbach, A. E.; Shitaraman, B.; Wilson, L. J. *J. Am. Chem. Soc.* **2005**, *127*, 799–805. (b) Bolskar, R. D.; Benedetto, A. F.; Hudebo, L. O.; Price, R. E.; Jackson, E. F.; Wallace, S.; Wilson, L. J.; Alford, J. M. *J. Am. Chem. Soc.* **2003**, *125*, 5471–5478. (c) Cagle, D. W.; Kennel, S. J.; Mirzadeh, S.; Alford, J. M.; Wilson, L. J. *Proc. Natl. Acad. Sci. U.S.A.* **1999**, *96*, 5182–5187.
- (6) (a) Bingel, C. *Chem. Ber.* **1993**, *126*, 1957–1959. (b) Hirsch, A.; Lamparth, I.; Karfunkel, H. R. *Angew. Chem., Int. Ed. Engl.* **1994**, *33*, 437–438. (c) Hirsch, A.; Lamparth, I.; Grösser, T.; Karfunkel, H. R. *J. Am. Chem. Soc.* **1994**, *116*, 9385–9386.
- (7) Feng, L.; et al. *J. Am. Chem. Soc.* **2005**, *127*, 17136–17137.
- (8) X-ray data were recorded by a Bruker SMART CCD diffractometer.
- (9) (a) Konarev, D. V.; Khasanov, S. S.; Otsuka, A.; Saito, G. *J. Am. Chem. Soc.* **2002**, *124*, 8520–8521. (b) Konarev, D. V.; Khasanov, S. S.; Saito, G.; Otsuka, A.; Yoshida, Y.; Lynbovskaya, R. N. *J. Am. Chem. Soc.* **2003**, *125*, 10074–10083. (c) Konarev, D. V.; Khasanov, S. S.; Vorontsov, I. I.; Saito, G.; Antipin, M. Y.; Otsuka, A.; Lynbovskaya, R. N. *Chem. Commun.* **2002**, 2548–2549.
- (10) Cheng, F.; Murata, Y.; Komatsu, K. *Org. Lett.* **2002**, *4*, 2541–2544.
- (11) Matsuo, Y.; Nakamura, E. *J. Am. Chem. Soc.* **2005**, *127*, 8457–8466.
- (12) The pyramidalization angles from the p-orbital axis vector analysis POAV ( $\theta_{\Delta\pi} - 90^\circ$ ) values provide a useful index of the local strain. See: Haddon, R. C. *Science* **1993**, *261*, 1545–1550.
- (13) For B3LYP, see: (a) Becke, A. D. *Phys. Rev. A* **1988**, *38*, 3098–3100. (b) Becke, A. D. *J. Chem. Phys.* **1993**, *98*, 5648–5652. (c) Lee, C.; Yang, W.; Parr, R. G. *Phys. Rev. B* **1988**, *37*, 785–789.
- (14) The single crystal of bisadduct (**A**) exhibits an unexpected strong ESR signal, even at low temperature. So far, no reasonable explanation is available for that. Further studies on its magnetic properties are still in process.

JA058390I